Electronic Supplementary Material (ESI) for Physical Chemistry Chemical Physics.

The effect of spin polarization on the electron transport of molecular wires with diradical character

Nicolás Ramos-Berdullas, Sara Gil-Guerrero, Ángeles Peña-Gallego and Marcos Mandado*

Department of Physical Chemistry, University of Vigo, Lagoas-Marcosende s/n, 36310, Vigo, Spain

1. Calculation of the electrical conductance from electron deformation orbitals (EDOs)

1.1. Single determinant wave functions

In the Landauer formula[1] the electric conductance, G, is obtained from the product of the quantum conductance, G_0, and the transmission function, T,

$$G = G_0 T \tag{S1}$$

where $G_0 = 2e^2/h$. This equation was originally obtained from scattering theory, but it can be also reached by linear-response theory[2] and the time-energy uncertainty relation approach to the electric conductance.[3] This approach is rooted in the origin of the quantum conductance and its relationship with the time-energy uncertainty principle. Bartra[4,5] derived the expression of G_0 by applying the uncertainty relation to the case of a free electron crossing a monodimensional conductor under the action of a finite bias voltage, ΔV. A generalization to interacting electrons subjected to the external potential created by the nuclei in a molecule gives rise to the following expression,[3]

$$G = \frac{E_{elec}^{(2)} \Delta q_{E-E}}{2h\Delta V} \tag{S2}$$

where, $\Delta q_{E\text{-}E}$ represents the net electronic charge transferred between electrodes upon the action of a bias voltage and $E_{elec}^{(2)}$ is the second order electrostatic energy. To get both

quantities, the difference between the electron density in the electrically perturbed and unperturbed states (ρ^{def}) has to be obtained. Eqns (S3) and (S4) provide expressions of $\Delta q_{E\text{-}E}$ and E_{elec} in terms of ρ^{def}, the latter including also higher order terms which are expected to be unimportant.

$$\Delta q_{E-E} = e\int_{\Omega_E} \rho^{def}(\vec{r})d\vec{r} \tag{S3}$$

$$E_{elec}^{(2)} \approx E_{elec} = e\int \rho^{def}(\vec{r})V(\vec{r})d\vec{r} \tag{S4}$$

It was proven that Eq (S2) can be transformed into Eq (S1) by expressing ρ^{def} with the so-called electron deformation orbitals (EDOs).[6] For a system perturbed by a constant electric field, EDOs can be obtained by diagonalization of the electron deformation density matrix. The electron deformation density matrix is defined as,

$$\mathbf{D}^{def} = \mathbf{D}^{l} - \mathbf{D}^{0} \tag{S5}$$

where, $\mathbf{D}^{l}$ and $\mathbf{D}^{0}$ are, respectively, density matrices for the perturbed and unperturbed systems on the basis of the unperturbed molecular orbitals. Then, the EDOs represent the eigenfunctions of $\mathbf{D}^{def}$, each with its corresponding eigenvalue. Denoting the eigenvector matrix by **U** and the set of unperturbed molecular orbitals by $\{\chi_i\}$, each EDO is given by,

$$\xi_i = \sum_j u_{ij}\chi_j \tag{S6}$$

They represent the eigenchannels for the electrically induced electron transport in molecules and are grouped in pairs of eigenfunctions with the same absolute eigenvalue but opposite sign. Positive and negative EDOs of a given pair, ξ_k^+ and ξ_k^-, are, respectively, electron and hole functions within the same electron transport channel, which is mathematically represented by the 2x2 matrix $\mathbf{\Theta}_k$,

$$\mathbf{\Theta}_k = n_k^{1/2}\begin{pmatrix} \xi_k^+ & 0 \\ 0 & i\xi_k^- \end{pmatrix} \tag{S7}$$

Thus, the total electron deformation density can be obtained from the traces of the $\mathbf{\Theta}_k$ matrix products,

$$\Delta\rho = 2\sum_{k=1}^{N_{CH}} \mathrm{Tr}\left(\mathbf{\Theta}_k^t \mathbf{\Theta}_k\right) \tag{S8}$$

Combining Eqs (S2), (S3), (S4) and (S6) leads, after some algebraic manipulations,[3] to the following expression for the electric conductance,

$$G = \frac{2e^2}{h} \mathrm{Tr}\left(\mathbf{t}^t \mathbf{t}\right) \tag{S9}$$

with the elements of the matrix **t** given by,

$$\mathbf{t}_{ij} = \left(\int \mathrm{Tr}\left(\mathbf{\Theta}_i^t \hat{\mathbf{r}}^{\mathrm{d}} \mathbf{\Theta}_i\right) d\tau \int_{\Omega_E} \mathrm{Tr}\left(\mathbf{\Theta}_j^t \mathbf{\Theta}_j\right) d\tau \right)^{1/2} \tag{S10}$$

In Eq (S8), $\hat{\mathbf{r}}^{\mathrm{d}}$ represents the position operator scaled to the distance, *d*, between the two points where the bias voltage is applied and the second integral on the rhs is restricted to the electrode region.

Since the EDOs are constructed as linear combinations of MOs, the role played by occupied and virtual orbitals on the electron transport can be analyzed. Moreover, the electron and hole densities associated with a given transmission channel can be represented in real space.

1.2 Multideterminant wave functions

For multideterminant wave functions, like the wave function obtained from the configuration interaction (CI) method,

$$\Psi_{CI} = \sum_{I=1}^{ND} c_I \Psi_I \tag{S11}$$

where Ψ_I represents one of *ND* possible determinants constructed from the combination of *N* electrons in *n* occupied and virtual Hartree-Fock spin orbitals, the electron density, ρ, may be expressed with the natural orbitals, ψ_i, and the corresponding occupation numbers, n_i.

$$\rho = \left\langle \Psi_{CI}^{\ *} \left| \hat{\rho} \right| \Psi_{CI} \right\rangle = \sum_{i=1}^{NNO} n_i \psi_i \qquad \text{(S12)}$$

These natural orbitals are the eigenvectors and eigenvalues of the electron density matrix. EDOs and electron transport channels given in Eqs (S6) and (S7) can then be constructed with these natural orbitals in the same way as in the single determinant case with occupied and virtual MOs. This does not imply any extra computational cost in the subsequent calculation of the electrical conductance.

2. Electrical conductance in open-shell singlet, triplet and broken-symmetry states

First, we show here how the electric conductance for open-shell singlet (OS), triplet (T) and broken symmetry (BS) states converge to the same value for perfect diradical chains.

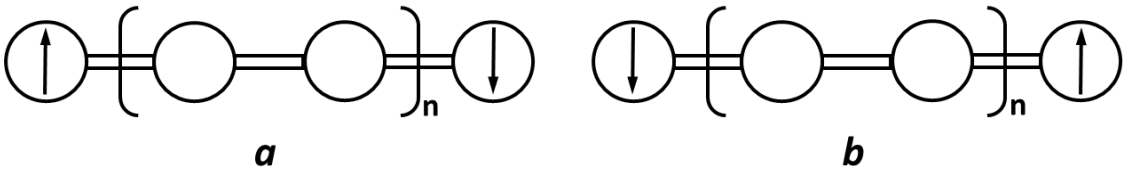

Fig. S1 Pictorial representation of the two BS states in a diradical chain with n+2 repeating units.

In Fig. S1, we can see a pictorial representation of the two possible BS states in a given diradical chain. To form these two BS states, the unpaired spin up and spin down electrons, localized at the chain ends, are exchanged, so that forming two degenerate states. Let's label these degenerate BS states as $\Psi_{BS}^{\uparrow\downarrow}$ (***a*** in Fig. S1) and $\Psi_{BS}^{\downarrow\uparrow}$ (***b*** in Figure

S1). They are not eigenstates of the spin operator squared, $\mathbf{S^2}$. Spin adapted configurations for the OS and one of the T states may be built from linear combinations of them.[7]

$$\Psi_S = 2^{-1/2}\left[\Psi_{BS}^{\uparrow\downarrow} - \Psi_{BS}^{\downarrow\uparrow}\right] \qquad \Psi_T = 2^{-1/2}\left[\Psi_{BS}^{\uparrow\downarrow} + \Psi_{BS}^{\downarrow\uparrow}\right] \tag{S13}$$

These states are then eigenstates of $\mathbf{S^2}$ and cannot be represented by just one single Slater determinant but the two determinants of the BS states. Alternatively, we can also represent the BS states as linear combinations of Ψ_S and Ψ_T

$$\Psi_{BS}^{\uparrow\downarrow} = 2^{-1/2}\left[\Psi_S + \Psi_T\right] \qquad \Psi_{BS}^{\downarrow\uparrow} = 2^{-1/2}\left[\Psi_T - \Psi_S\right] \tag{S14}$$

We can go on with any of the two BS states represented above, both will lead us to the same result. Applying the density operator on state $\Psi_{BS}^{\uparrow\downarrow}$ and considering the orthogonality of OS and T states, we have,

$$\left\langle \Psi_{BS}^{\uparrow\downarrow *} \left| \hat{\rho} \right| \Psi_{BS}^{\uparrow\downarrow} \right\rangle = 2^{-1}\left[\left\langle \Psi_S{}^* \left| \hat{\rho} \right| \Psi_S \right\rangle + \left\langle \Psi_T{}^* \left| \hat{\rho} \right| \Psi_T \right\rangle\right] \tag{S15}$$

which tell us the electron density of the BS states is the average of the OS and T electron densities. We can then obtain the electron density of the OS state, which is not accessible from a single determinant DFT calculation, indirectly from the T and BS states.

$$\left\langle \Psi_S{}^* \left| \hat{\rho} \right| \Psi_S \right\rangle = 2\left\langle \Psi_{BS}^{\uparrow\downarrow *} \left| \hat{\rho} \right| \Psi_{BS}^{\uparrow\downarrow} \right\rangle - \left\langle \Psi_T{}^* \left| \hat{\rho} \right| \Psi_T \right\rangle \tag{S16}$$

In the case of the T, we cannot obtain the state given in Eq (S13) but any of the other two degenerate states with two spin up or spin down electrons, respectively, from a single determinant unrestricted DFT calculation.

The one-electron density matrix for the OS can be represented on the basis of the so-called magnetic orbitals from the BS state or the spin-orbitals from the T. Using the former, the one-electron density matrix for the OS is given by,

$$\mathbf{D_S} = 2\mathbf{D_{BS}} - \mathbf{O}^{\mathbf{t}}_{\mathbf{T\rightarrow BS}}\mathbf{D_T}\mathbf{O}_{\mathbf{T\rightarrow BS}} \tag{S17}$$

where $\mathbf{O}_{\mathbf{T}\rightarrow\mathbf{BS}}$ is the orbital transformation matrix from the T spin orbitals to the BS magnetic orbitals. With the density matrix before and after the application of the perturbation, we can proceed with the calculation of the electrical conductance following the method explained in section 1.1. However, in strongly diradical chains, where the overlap between the spin up and spin down magnetic orbitals is negligible,[8] the differences in the electron density and the energy of the OS, T and BS states are also negligible. As proof, we have represented in Fig. S2 the electrical conductance for the BS and T states in the series of dimethylene polyphenylene, dimethylene polyfuran and dimethylene polythiophene.

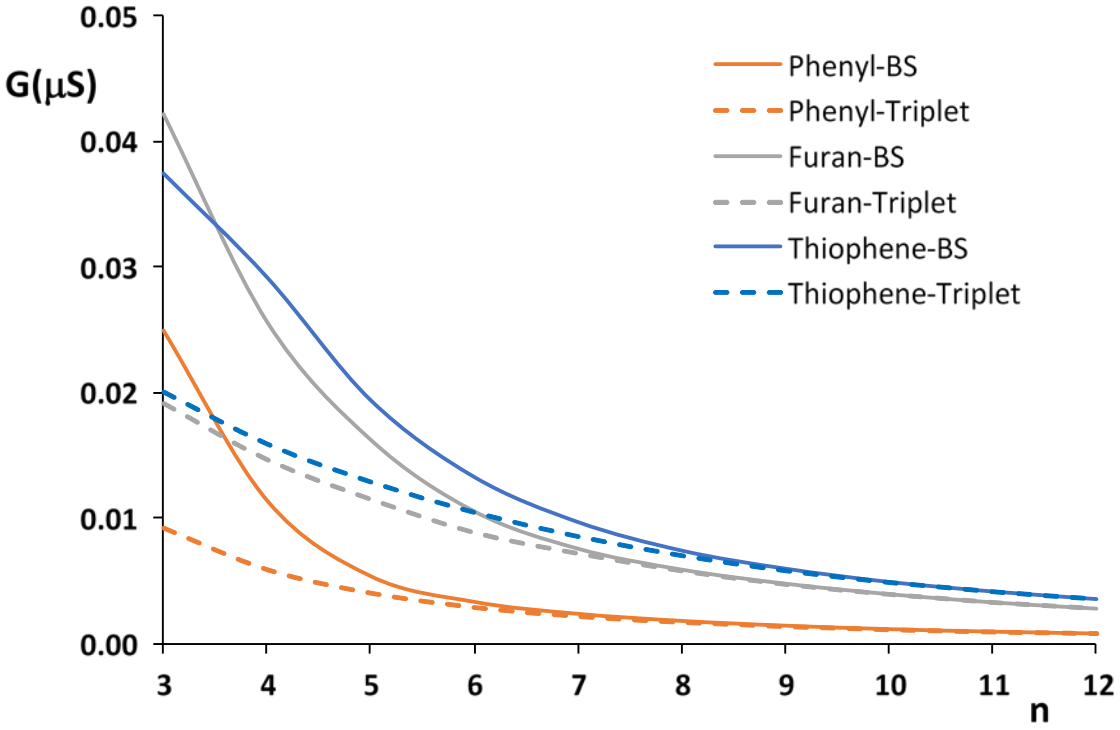

Fig. S2 Electrical conductance vs the number of aromatic units for the BS (solid lines) and T (dashed lines) states of dimethylene polyphenylene (orange), dimethylene polyfurane (grey) and dimethylene polythiophene (blue) chains.

As can be observed, the conductance profiles are identical for long chains with strong diradical character. Taking into account that BS-UKS-DFT performs well in these cases,

we have analyzed in the body of the letter directly the electrical conductance in the BS state instead of the OS.

3. Energy gaps between different spin states

In this section, the energies of the closed-shell singlet (CS), BS and T states are compared in three different tables for the organic polymeric (Table S1), quinoid-cumulenes (Table S2), and graphene strips (Table S3). For perfect diradical chains the BS-T energy gap is negligible. This happens in dimethylene polyphenylene with n > 4, dimethylene polyfurane with n > 7 and dimethylene polythiophene with n > 8, in agreement with the conductance curves represented in Fig. S2. In quinoid-cumulenes, the diradical character is significantly lower but the BS is the lowest energy state for all the chains. In graphene strips with N = 5, no BS state was found and the T state is significantly less stable than the CS. In strips with N = 7 and N = 9, the BS state is always more stable than the CS, and an almost perfect diradical character is reached for chains with n > 10 and n > 5, respectively.

Table S1. Energies for the closed-shell (**CS**), broken-symmetry (**BS**) and triplet (**T**) lower energy states in dimethylene polyphenylene (**Phenyl**), dimethylene polyfurane (**Furan**) and dimethylene polythiophene (**Thiophene**) chains. Absolute energies in Hartrees are given for **CS**, whereas those of **BS** and **T** are relative to **CS** and given in eV.

Phenyl	CS	BS	T
3	-1311.04796	-0.390	-0.351
4	-1542.01020	-0.728	-0.722
5	-1772.97874	-0.910	-0.909
6	-2003.95141	-0.986	-0.986
7	-2234.92569	-1.014	-1.017
8	-2465.90061	-1.030	-1.030
9	-2696.87559	-1.038	-1.038
10	-2927.85094	-1.044	-1.044
11	-3158.82605	-1.047	-1.047

12	-3389.80151	-1.051	-1.051
Furan			
3	-1304.58508	-0.004	0.301
4	-1533.43531	-0.125	-0.015
5	-1762.28692	-0.301	-0.260
6	-1991.13987	-0.461	-0.445
7	-2219.99457	-0.589	-0.583
8	-2448.85093	-0.669	-0.666
9	-2677.70845	-0.725	-0.724
10	-2906.56670	-0.759	-0.759
11	-3135.42553	-0.776	-0.776
12	-3364.28440	-0.795	-0.795
Thiophene			
3	-2273.55860	-0.001	0.390
4	-2825.39958	-0.051	0.106
5	-3377.24151	-0.179	-0.115
6	-3929.08406	-0.324	-0.297
7	-4480.92749	-0.457	-0.446
8	-5032.77213	-0.563	-0.558
9	-5584.61809	-0.635	-0.633
10	-6136.46511	-0.679	-0.678
11	-6688.31276	-0.706	-0.705
12	-7240.16078	-0.719	-0.719

Table S2. Energies for the closed-shell (**CS**), broken-symmetry (**BS**) and triplet (**T**) lower energy states in quinoid-cumulenes with phenyl (**QDC**) and anthracene (**AC**) as central aromatic units. Absolute energies in Hartrees are given for **CS**, whereas those of **BS** and **T** are relative to **CS** and given in eV.

QDC	CS	BS	T
1	-841.68742	-0.060	-0.004
2	-993.83739	-0.074	-0.031
3	-1145.99180	-0.084	-0.051
4	-1298.14791	-0.092	-0.067
5	-1450.30477	-0.095	-0.079
AC			

1	-1148.62190	-0.008	0.113
2	-1300.77173	-0.018	0.069
3	-1452.92592	-0.028	0.041
4	-1605.08179	-0.037	0.018
5	-1757.23845	-0.045	0.000

Table S3. Energies for the closed-shell (**CS**), broken-symmetry (**BS**) and triplet (**T**) lower energy states in armchair graphene strips with N = 5 (**Naphthalene**), N = 7 (**Anthracene**) and N = 9 (**Tetracene**). For N = 9 and n ≤ 8, absolute energies in Hartrees are given for **CS**, whereas those of **BS** and **T** are relative to **CS** and given in eV. For N = 9 and n > 8, calculations of **CS** did not converge and the data for **BS** correspond to absolute energies given in Hartrees, whereas those of **T** are relative to **BS** and given in eV.

Naphtalene	**CS**	**BS**	**T**
2	-769.4602	0.000	1.877
3	-1152.9990	0.000	1.401
4	-1536.5381	0.000	1.162
5	-1920.0774	0.000	1.023
6	-2303.6166	0.000	0.934
7	-2687.1559	0.000	0.873
8	-3070.6952	0.000	0.831
9	-3454.2346	0.000	0.801
10	-3837.7739	0.000	0.778
11	-4221.3132	0.000	0.762
12	-4604.8525	0.000	0.749
13	-4988.3918	0.000	0.739
14	-5371.9311	0.000	0.732
15	-5755.4705	0.000	0.726
16	-6139.0098	0.000	0.722
17	-6522.5491	0.000	0.718
18	-6906.0884	0.000	0.715
19	-7289.6277	0.000	0.713
20	-7673.1671	0.000	0.712
Anthracene			
2	-1075.5767	0.000	0.829
3	-1611.5864	-0.021	0.330
4	-2147.5985	-0.106	0.055

5	-2683.6120	-0.201	-0.123
6	-3219.6265	-0.287	-0.249
7	-3755.6420	-0.358	-0.340
8	-4291.6581	-0.415	-0.405
9	-4827.6749	-0.457	-0.452
10	-5363.6921	-0.488	-0.485
11	-5899.7097	-0.510	-0.508
12	-6435.7275	-0.525	-0.524
13	-6971.7455	-0.536	-0.535
14	-7507.7636	-0.543	-0.543
15	-8043.7818	-0.549	-0.549
16	-8579.8000	-0.553	-0.553
17	-9115.8183	-0.556	-0.556
18	-9651.8366	-0.559	-0.559
19	-10187.8550	-0.561	-0.561
20	-	-	-
Tetracene			
2	-1381.6923	-0.063	0.233
3	-2070.1767	-0.293	-0.221
4	-2758.6668	-0.464	-0.443
5	-3447.1602	-0.562	-0.555
6	-4135.6555	-0.613	-0.611
7	-4824.1518	-0.640	-0.639
8	-5512.6486	-0.655	-0.655
9		-6201.1700	0.000
10		-6889.6673	0.000
11		-7578.1646	0.000
12		-8266.6619	0.000
13		-8955.1593	0.000
14		-9643.6566	0.000
15		-10332.1539	0.000
16		-11020.6512	0.000
17		-11709.1485	0.000
18		-12397.6458	0.000
19		-13086.1432	0.000

20	-13774.6402	-0.008

4. Diradical character in graphene strips from CASSCF(2,2) calculations

In this section, the diradical character in the different graphene strips is compared using minimal active space CASSCF calculations with the help of the pseudo-π approach.[9] The pseudo-π approach exploits the one-to-one symmetry correspondence between the π orbitals of an sp2-carbon structure and the σ orbitals in an equivalent hydrogen structure. In practice, the carbon atoms in a geometrically optimized sp2-carbon structure are replaced by hydrogens speeding up considerably the calculations. The resulting pseudo-π structure has MOs with the same symmetry properties as the π MOs of the real carbon structure.

The number of effectively unpaired electrons (N_U)[10] measures the radical character, being comprised between 0 and 2 in the case of partially diradical structures. This index is obtained from the occupation numbers, n_i, of the natural orbitals within the active space, AS, in a CASSCF calculation.

$$N_U = \sum_{i \in AS} n_i^2 \left(2 - n_i\right)^2 \qquad \text{(S17)}$$

In Table S4, the N_U values for the pseudo-π structures of the graphene strips are collected. They clearly reflect there is no diradical character in the strips with N = 5, whereas strips with N = 9 are strongly diradical even in relatively short chains. Strips with N = 7 represent an intermediate situation. All of this is in agreement with the BS-UKS-DFT energy gaps shown in the previous section.

Table S4. N_U values obtained at the CASSCF(2,2) level using the pseudo-π approach for the armchair graphene strips with N = 5 (**Naphthalene**), N = 7 (**Anthracene**) and N = 9 (**Tetracene**).

	Naphthalene	**Anthracene**	**Tetracene**
2	0.06	0.06	0.32
3	0.06	0.05	1.52
4	0.06	0.03	1.89
5	0.06	1.05	1.97
6	0.06	1.86	1.99
7	0.01	1.94	2.00
8	0.06	1.97	2.00
9	0.06	1.99	2.00
10	0.06	1.99	2.00
11	0.06	2.00	2.00
12	0.06	2.00	2.00
13	0.06	2.00	2.00
14	0.00	2.00	2.00
15	0.00	2.00	2.00
16	0.00	2.00	2.00
17	0.00	2.00	2.00
18	0.00	2.00	2.00
19	0.00	2.00	2.00
20	0.00	2.00	2.00

5. Tetraphenyl cumulenes

In this section, we present calculations carried out for the tetraphenyl cumulenes depicted in Fig. S3.

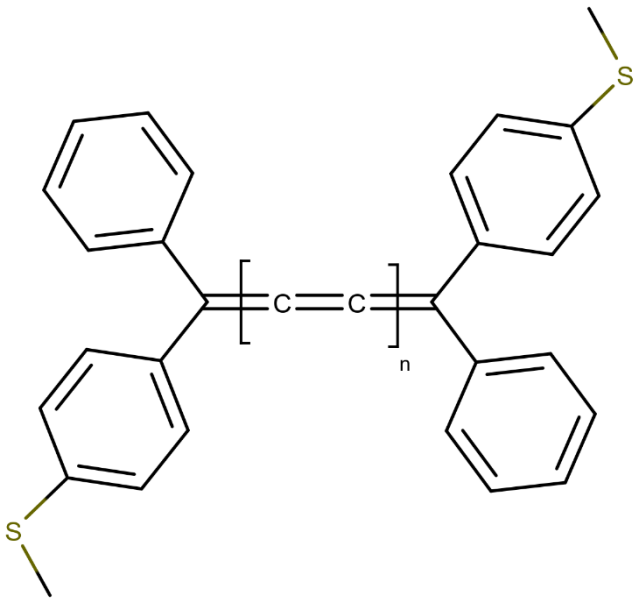

Fig. S3 Tetraphenyl cumulene chains studied in references 11 and 12 **C4** (n=1), **C6** (n=2) and **C8** (n=3).

The electron transport in these systems has been studied experimentally using STM, obtaining an unexpected increase of the electrical conductance with the length of the cumulene chain.[11,12] Transmission calculations using NEGF-DFT reproduce the experimental behavior.[11,12] Herein, we have first investigated if this behavior is connected to diradical character. In Table S5, the energies of the CS, BS and T states are collected. CS state is significantly more stable than T state in all cases, so that the calculations for the BS state converge to the CS. Therefore, these systems do not seem to display a perceptible diradical character and the increase of the electrical conductance with the length may be associated with other electronic or geometrical features.

Table S5. Energies for the closed-shell (**CS**), broken-symmetry (**BS**) and triplet (**T**) lower energy states in the tetraphenyl cumulenes depicted in Figure S4. Absolute energies in Hartrees are given for **CS**, whereas those of **BS** and **T** are relative to **CS** and given in eV.

	CS	**BS**	**T**
C4	-1953.4640	0.000	1.019
C6	-2029.5845	0.000	0.656

C8	-2105.7080	0.000	0.464

Herein, the electrical conductance obtained for the same chains using EDOs is depicted in Fig. S4. The calculations were performed on geometrically optimized chains attached by the sulphur atoms to clusters containing twenty gold atoms. The bond distances between sulphurs and the apical centers of the clusters were also optimized as well as the S-Au-C bond angles. As can be observed, a small increase of the conductance with the length of the central cumulene chain is also predicted using EDOs.

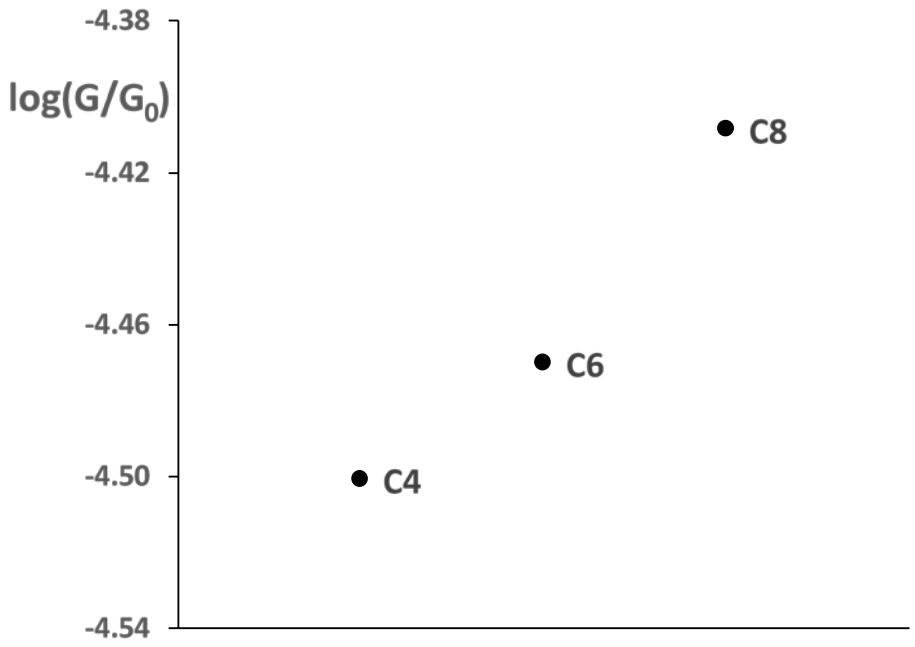

Fig. S4 Electrical conductance calculated at a voltage of 100 mV for the tetraphenyl cumulene chains depicted in Fig. S3 attached to clusters of 20 gold atoms. The conductance is given relative to the quantum conductance G_0 using a logarithmic scale.

References

1 R. Landauer, Spatial Variation of Currents and Fields Due to Localized Scatterers in Metallic Conduction, *IBM J. Res. Dev.*, 1957, **1**, 223.

2 H. D. Cornean, A. Jensen and V. J. Moldoveanu, *Math. Phys.*, 2005, **46**, 042106.

3 N. Ramos-Berdullas, S. Gil-Guerrero and M. Mandado, Transmission channels in the time-energy uncertainty relation approach to molecular conductance: symmetry rules for the electron transport in molecules, *Int. J. Quantum Chem.*, 2018, **118**, e25651.

4 I. P. Batra, Origin of conductance quantization, *Surf. Sci.*, 1998, **395**, 43.

5 I. P. Batra, From uncertainty to certainty in quantum conductance of nanowires, *Solid State Commun.*, 2002, **124**, 463.

6 M. Mandado, and N. Ramos-Berdullas, Analyzing the electric response of molecular conductors using “electron deformation” orbitals and occupied-virtual electron transfer, *J. Comput. Chem.*, 2014, **35**, 1261.

7 J. M. Mouesca Density Functional Theory–Broken Symmetry (DFT–BS) Methodology Applied to Electronic and Magnetic Properties of Bioinorganic Prosthetic Groups. In: Metalloproteins. Methods in Molecular Biology (Methods and Protocols), vol 1122, Fontecilla-Camps J.; Nicolet Y., Humana Press, Totowa, NJ, 2014.

8 F. Neese, Definition of corresponding orbitals and the diradical character in broken symmetry DFT calculations on spin coupled systems, *J. Phys. Chem. Sol.*, 2004, **65** 781.

9 P. W. Fowler and E. Steiner, E. Pseudo-π currents: rapid and accurate visualisation of ring currents in conjugated hydrocarbons, *Chem. Phys. Lett.*, 2002, **364**, 259.

10 M. Head-Gordon, Characterizing unpaired electrons from the one-particle density matrix, *Chem. Phys. Lett.*, 2003, **372**, 508.

11 W. Xu, E. Leary, S. Hou, S. Sangtarash, M. T. Gonzalez, G. Rubio-Bollinger, Q. Wu, H. Sadeghi, L. Tejerina, K. E. Christensen, N. Agrait, S. J. Higgins, C. J. Lambert, R. J. Nichols and H. L. Anderson, Unusual Length Dependence of the Conductance in Cumulene Molecular Wires. *Angew. Chem. Int. Ed.*, 2019, **58**, 8378.

12 Y. Zang, T. Fu, Q. Zou, F: Ng, H. Li, M. L. Steigerwald, C. Colin Nuckolls, L. Venkataraman, Cumulene Wires Display Increasing Conductance with Increasing Length, *Nano Lett.*, 2020, DOI: 10.1021/acs.nanolett.0c03794.